JCI The Journal of Clinical Investigation

VEGF-C and aortic cardiomyocytes guide coronary artery stem development

Heidi I. Chen, … , Kari Alitalo, Kristy Red-Horse

J Clin Invest. 2014;124(11):4899-4914. https://doi.org/10.1172/JCI77483.

Research Article **Vascular biology**

Coronary arteries (CAs) stem from the aorta at 2 highly stereotyped locations, deviations from which can cause myocardial ischemia and death. CA stems form during embryogenesis when peritruncal blood vessels encircle the cardiac outflow tract and invade the aorta, but the underlying patterning mechanisms are poorly understood. Here, using murine models, we demonstrated that VEGF-C–deficient hearts have severely hypoplastic peritruncal vessels, resulting in delayed and abnormally positioned CA stems. We observed that VEGF-C is widely expressed in the outflow tract, while cardiomyocytes develop specifically within the aorta at stem sites where they surround maturing CAs in both mouse and human hearts. Mice heterozygous for islet 1 (*Isl1*) exhibited decreased aortic cardiomyocytes and abnormally low CA stems. In hearts with outflow tract rotation defects, misplaced stems were associated with shifted aortic cardiomyocytes, and myocardium induced ectopic connections with the pulmonary artery in culture. These data support a model in which CA stem development first requires VEGF-C to stimulate vessel growth around the outflow tract. Then, aortic cardiomyocytes facilitate interactions between peritruncal vessels and the aorta. Derangement of either step can lead to mispatterned CA stems. Studying this niche for cardiomyocyte development, and its relationship with CAs, has the potential to identify methods for stimulating vascular regrowth as a treatment for cardiovascular disease.

VEGF-C and aortic cardiomyocytes guide coronary artery stem development

Heidi I. Chen,[1] Aruna Poduri,[1] Harri Numi,[2] Riikka Kivela,[2] Pipsa Saharinen,[2] Andrew S. McKay,[1] Brian Raftrey,[1] Jared Churko,[3] Xueying Tian,[4] Bin Zhou,[4] Joseph C. Wu,[3] Kari Alitalo,[2] and Kristy Red-Horse[1]

[1]Department of Biology, Stanford University, Stanford, California, USA. [2]Wihuri Research Institute and Translational Cancer Biology Program, University of Helsinki, Biomedicum Helsinki, Helsinki, Finland. [3]Department of Medicine, Division of Cardiology, Stanford University, Stanford, California, USA. [4]Key Laboratory of Nutrition and Metabolism, Institute for Nutritional Sciences, Shanghai Institutes for Biological Sciences, Graduate School of the Chinese Academy of Sciences, Chinese Academy of Sciences, Shanghai, China.

Coronary arteries (CAs) stem from the aorta at 2 highly stereotyped locations, deviations from which can cause myocardial ischemia and death. CA stems form during embryogenesis when peritruncal blood vessels encircle the cardiac outflow tract and invade the aorta, but the underlying patterning mechanisms are poorly understood. Here, using murine models, we demonstrated that VEGF-C–deficient hearts have severely hypoplastic peritruncal vessels, resulting in delayed and abnormally positioned CA stems. We observed that VEGF-C is widely expressed in the outflow tract, while cardiomyocytes develop specifically within the aorta at stem sites where they surround maturing CAs in both mouse and human hearts. Mice heterozygous for islet 1 (*Isl1*) exhibited decreased aortic cardiomyocytes and abnormally low CA stems. In hearts with outflow tract rotation defects, misplaced stems were associated with shifted aortic cardiomyocytes, and myocardium induced ectopic connections with the pulmonary artery in culture. These data support a model in which CA stem development first requires VEGF-C to stimulate vessel growth around the outflow tract. Then, aortic cardiomyocytes facilitate interactions between peritruncal vessels and the aorta. Derangement of either step can lead to mispatterned CA stems. Studying this niche for cardiomyocyte development, and its relationship with CAs, has the potential to identify methods for stimulating vascular regrowth as a treatment for cardiovascular disease.

Introduction

The vascular beds of each individual organ are shaped to optimize blood flow through the different tissues of the body. In the heart, 2 coronary artery (CA) stems are located at specific sites on the aorta, one at the right sinus and one at the left sinus of the aortic valve (Figure 1A). The stem sites are positioned to efficiently deliver oxygenated blood to the ventricular myocardium. Congenital anomalies causing stems to arise at abnormal sites can cause myocardial ischemia and sometimes lead to sudden death (1, 2). Most dramatic is when CAs stem from the pulmonary artery, which carries deoxygenated blood. Usually fatal if left untreated, this malformation (anomalous left CA from the pulmonary artery [ALCAPA]) requires surgery soon after birth and often entails lifelong complications (3, 4). Despite the clinical relevance of proper stem formation, the mechanisms that dictate this process during embryonic development are unknown.

Much of what we have learned about CA stem formation is from studies performed in chick embryos (5–8). For over a century, observations made using general histological stains suggested that CA stems arise by endothelial budding off the aorta (9, 10). A breakthrough in our understanding came from careful histological analyses and transplantation studies in chicks showing that, instead of outward budding, blood vessels that surround the cardiac outflow tract — termed peritruncal vessels — grow inward and fuse with the aorta (6, 7, 11). Recent lineage tracing has suggested a similar invasion process in the mammalian heart (12). These studies led to the current model in which peritruncal vessels first invade and anastomose with the aorta at multiple sites around its base, before remodeling into 2 larger-bore vessels at the right and left stem sites (Figure 1A and ref. 5). In chicks, this process requires PDGF, FGF, and VEGF-B, since inhibiting these molecules during coronary development decreases the number of stems formed (5, 13, 14). In mice, the remodeling of CA stems requires regulation of BMP signaling by BMP-binding endothelial regulator (BMPER) (15). However, the specific mechanisms patterning their spatial arrangement on the aorta are unknown.

In all species studied, including humans, correct positioning of CA stems depends on proper morphogenesis of the outflow tract. Inhibition of cardiac neural crest (16) and second heart field development (17) results in outflow tract septation and rotation defects that are associated with abnormally placed CA stems on the aorta. Interestingly, CAs do not connect with the pulmonary artery under these conditions, even in the presence of dramatic morphological defects. Similar phenotypes have been observed in *Cx43*-, *Tbx1*-, and perlecan-null mice (18–20) as well as in retinoic acid–treated embryos (21). Coronary stems are also abnormal in human hearts with rotation defects called

Authorship note: Heidi I. Chen and Aruna Poduri contributed equally to this work.
Conflict of interest: Kari Alitalo is a consultant for Herantis Pharma Ltd. Joseph C. Wu is a consultant for the publically traded company Ivivi.
Submitted: June 10, 2014; **Accepted:** August 28, 2014.
Reference information: *J Clin Invest*. 2014;124(11):4899–4914. doi:10.1172/JCI77483.

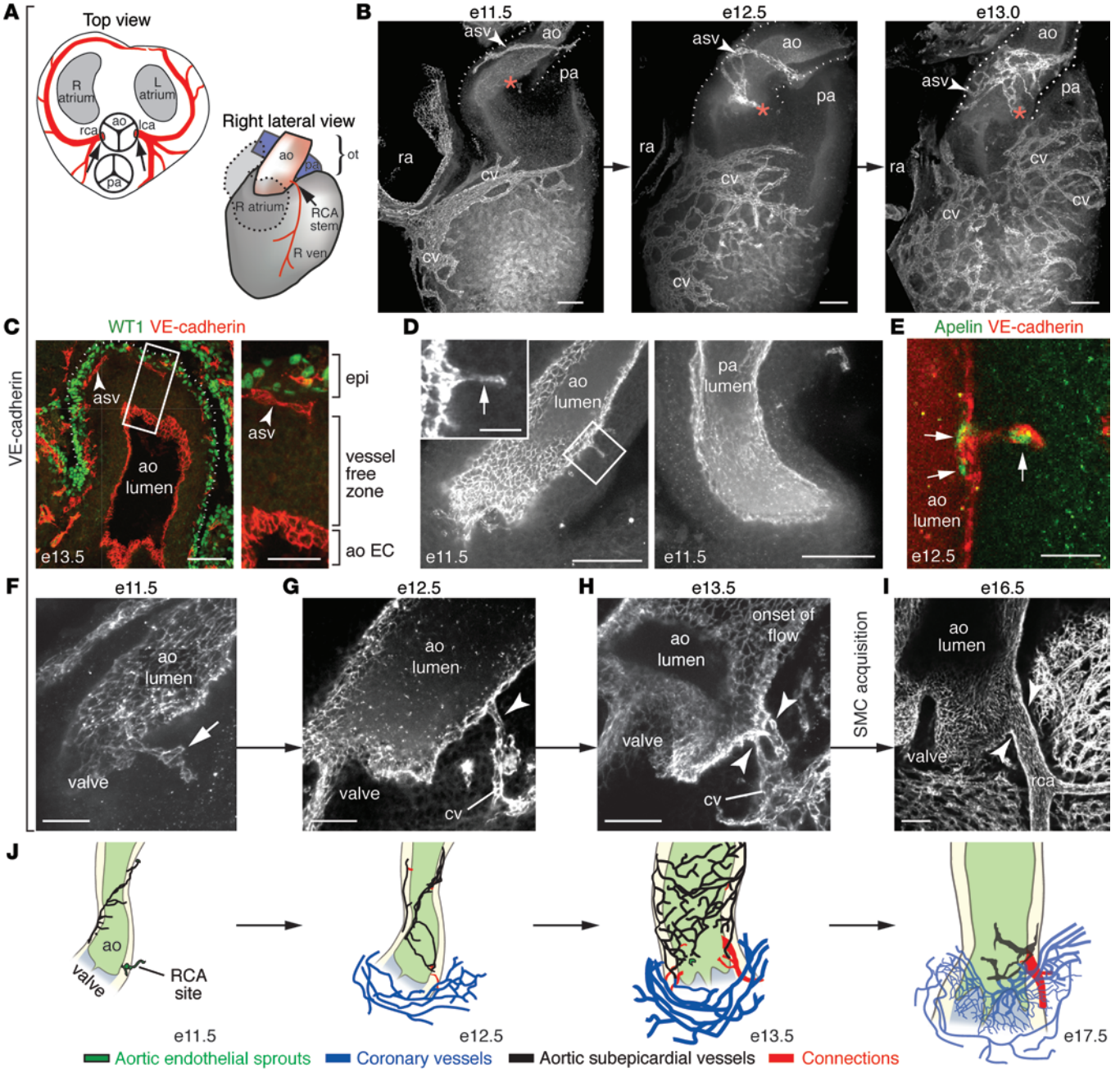

Figure 1. CA stem development in mice. (**A**) Schematics showing top and right lateral views of the heart, including CA stem locations (black arrows). (**B**) Confocal images of the right lateral side of hearts from the indicated embryonic days labeled for VE-cadherin. Coronary vessels (cv) and ASVs (arrowheads) grow toward the future right CA stem site (red asterisk) on the aorta (ao, dotted lines). (**C**) Tissue section through the aorta showing the presence of ASVs (red, arrowheads) directly beneath the epicardium (WT1$^+$, green) and a vessel-free region around the aorta. The right panel is a high-magnification view of the boxed region. (**D**) Luminal endothelial cells lining the aorta, but not the pulmonary artery (pa), form sprouts (arrow). Inset is a high-magnification view of the boxed region. (**E**) *Apelin-nlacZ* expression (green, arrows) in VE-cadherin$^+$ (red) aortic endothelium and adjacent sprouts. (**F**–**I**) Image projections of the CA stem site. (**F**) Small endothelial extensions from the aorta (arrow). (**G**) Initial interactions between coronary vessels and the aorta consist of thin, single-celled connections (arrowhead). (**H**) Multiple, lumenized connections that receive blood flow (arrowheads) develop at the future stem site and begin to acquire smooth muscle cell (SMC) coverage. (**I**) The mature pattern is a single, larger bore vessel stemming from the right coronary sinus (arrowheads) directly distal to the valves. (**J**) CA stem development. epi, epicardium; EC, endothelial cell; L atrium, left atrium; lca, left CA; ot, outflow tract; ra, right atrium; R atrium, right atrium; r ven, right ventricle; RCA, right CA. Scale bars: 100 μm (**B**–**D**); 50 μm (**F**–**I**); 25 μm (**E**, right panel in **C**, and inset in **D**).

transposition of the great arteries (TGA) (22). Thus, the mechanisms patterning CAs on the aorta are altered when outflow tract rotation is disturbed, but the factors restricting them from the pulmonary artery remain intact.

Our study provides insight into the factors around the outflow tract and aorta that facilitate CA stem formation at the proper location. VEGF-C is highly expressed around the outflow tract and is required for normally patterned stems because it attracts

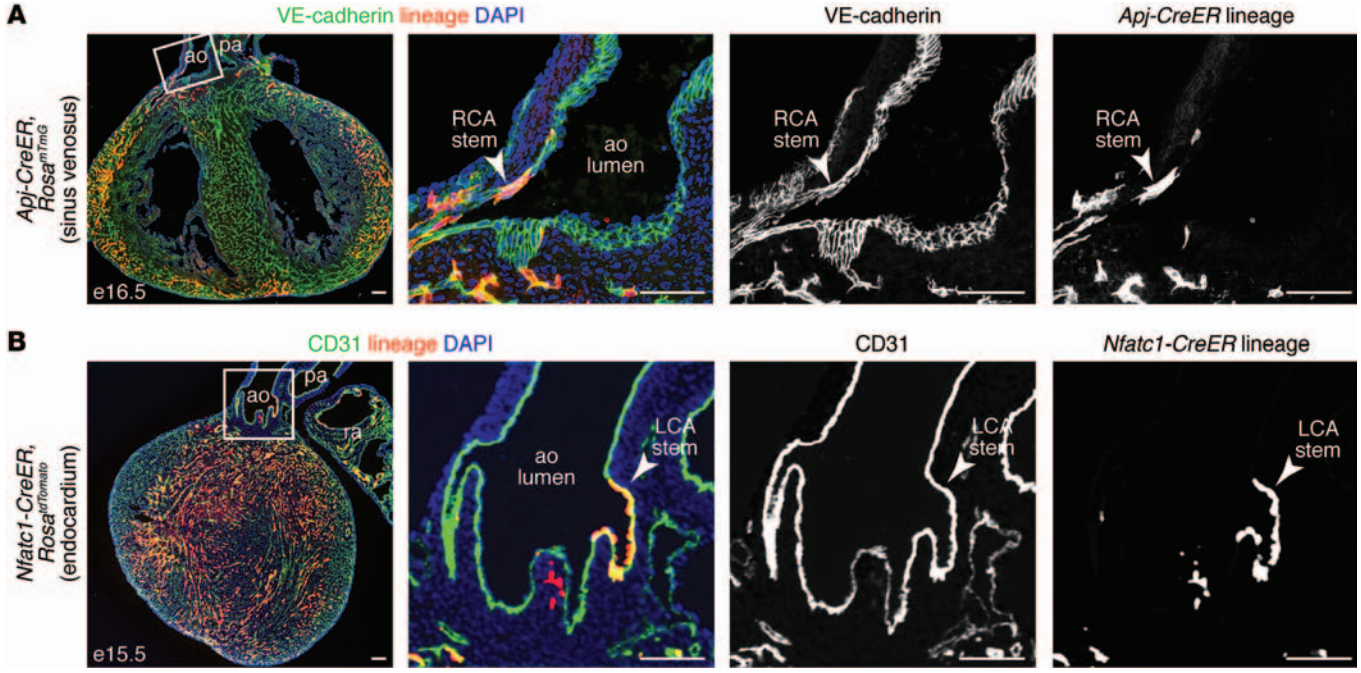

Figure 2. The sinus venosus and endocardium both contribute to CA stems. Tissue sections of hearts immunostained with endothelial markers (VE-cadherin or CD31) and a nuclear dye (DAPI). Lineage-traced cells (arrowheads) are present in CA stems from (**A**) *Apj-CreER, Rosa*^{mTmG} and (**B**) *Nfatc1-CreER, Rosa*^{tdTomato} embryos. Right panels are high-magnification views of the boxed regions. Scale bars: 100 μm.

robust vessel growth near the presumptive stem sites on the aorta. Although necessary for the proper establishment of peritruncal vessels, VEGF-C expression throughout the aorta and pulmonary artery suggests that it does not specify the exact location of the stem sites. Instead, we found that cardiomyocytes, a highly angiogenic cell type (23, 24), are present specifically in the wall of the aorta, but not in the pulmonary artery, and that they surround developing stems in both mouse and human hearts. Heterozygosity for islet 1 (*Isl1*) decreases aortic cardiomyocytes and leads to delayed, abnormally targeted stems. Misplaced stems remain tightly associated with aortic cardiomyocytes on hearts with outflow tract rotation defects, and cardiomyocytes induce ectopic endothelial connections with the pulmonary artery in vitro. Our data suggest that VEGF-C first induces vascular expansion around the outflow tract, followed by cardiomyocyte-assisted vessel growth specifically at the CA stem sites. Inhibition of either mechanism results in mistargeted CA stems. Understanding this process will begin to shed light on the molecular defects that cause congenitally misplaced CA stems and could suggest methods of generating new CAs following injury or disease.

Results

CA stem formation in the mammalian heart. A stepwise, high-resolution characterization of CA stem development has not been performed in the mammalian heart. Therefore, we used whole-mount confocal microscopy to image blood vessels in mouse hearts isolated from E10.5 to birth. We found that peritruncal vessels surrounding the aortas and pulmonary arteries first appeared at E11.5 and arose from 2 different locations. First, coronary vessels migrated toward the base of the outflow tract as they grew over and into the heart (Figure 1B). Second, a previously undescribed plexus was detected on the aorta, which began as a single vessel that circled its lateral side before expanding at later developmental stages (Figure 1B and Supplemental Figure 1; supplemental material available online with this article; doi:10.1172/JCI77483DS1). These vessels developed directly beneath the aortic epicardium (Figure 1C) and were therefore termed aortic subepicardial vessels (ASVs). Similar vessels were seen occasionally in the analogous region of the pulmonary artery but with much less frequency and at lower densities (data not shown). ASVs appeared to be blood vessels, since they contained erythrocytes (Supplemental Figure 2A) and connected to aortic endothelium (see below). However, a subset of early ASV endothelial cells was positive for the lymphatic marker PROX1 but negative for the mature lymphatic marker LYVE-1 (Supplemental Figure 2, B and C). LYVE-1$^+$ vessels appeared on the aorta much later at E16.5 (Supplemental Figure 2D). Both coronary vessels and ASVs expanded as development progressed (Figure 1B), but only coronary vessels persisted while ASVs mostly disappeared by E17.5 (Supplemental Figure 1). Thus, peritruncal vessels surrounding the outflow tract are composed of developing coronary vessels and ASVs.

Prior to any anastomosis event between the aorta and peritruncal vessels, the aortic endothelium often extended sprouts (Figure 1, D and E, and Supplemental Figure 3A), which never appeared on the pulmonary artery (Figure 1D and Supplemental Figure 3A). Sprouts were frequently 1 cell extending into the medial layer surrounding the aorta (Figure 1, D and E), but those consisting of 2 to 5 cells were also observed (Figure 1F). Extending cells and adjacent aortic endothelial cells expressed apelin, a marker for sprouting endothelium (Figure 1E). These sprouts were independent of coronary vessel or ASV development, since they still formed when peritruncal vessels were inhibited by an early

injection of the VEGFR antagonist axitinib (Supplemental Figure 3B). The presence of aortic sprouts is in contrast to that in avian experiments, which report only the ingrowth of peritruncal vessels, with no budding of the aorta. This could be due to species differences or our use of high-resolution confocal microscopy, which can detect single-cell processes deep within tissue. It does not appear that the sprouts robustly contributed to the stem, since they were very small (1–5 cells) and did not grow extensively in the absence of peritruncal vessels (Supplemental Figure 3B). Taken together, these observations suggest that the environment surrounding the aorta is angiogenic, while the analogous region on the pulmonary artery is not, but that ingrowth of coronary vessels is the primary mechanism of stem formation.

Connections between the aorta and peritruncal vessels emerged between E12.5 and E13.5 and formed at locations that include both future CA stem sites (Figure 1G) and various points higher on the artery (Supplemental Figure 3A and Supplemental Figure 4). Connections never formed on the pulmonary artery (Supplemental Figure 3A). Initial fusions consisted of lumenless, single-cell thick bridges (Figure 1G). If these connections were positioned at the future stem site adjacent to the valve, they expanded in the next developmental stage. Expansion involved the formation of multiple, clustered connections with increased diameters that began to receive blood from the aorta (Figure 1H and Supplemental Figure 5A). The stem site was not located at the exact same spot in each heart but occurred within a range at or above where the valve leaflets converge (Supplemental Figure 6, A and B). At E14.5, vascular smooth muscle development was initiated around the CA stems (Supplemental Figure 5B), and, by E16.5, the mature stem morphology was seen (Figure 1I). In summary, the process of CA stem formation in the mammalian heart includes anastomoses of peritruncal vessels with a sprouting aortic endothelium, followed by the remodeling and maturation of only those connections at the stem sites (Figure 1J and Supplemental Figure 4).

Coronary vessels originate from at least 3 progenitor populations, the sinus venosus (25, 26), endocardium (25, 27), and proepicardium (28), the latter of which may first transition through the former cell types (28). We next performed Cre recombinase–based lineage tracing with Cre lines expressed in the sinus venosus and endocardium to assess their contribution to CA stems. Mice containing either the *Rosa*^{mTmG} or *Rosa*^{tdTomato} Cre reporter alleles were crossed with *Apj-CreER* or *Nfatc1-CreER* transgenic mice to lineage label the sinus venosus and endocardium, respectively. When analyzed at later embryonic stages, stems contained lineage-labeled cells from both *Apj-CreER* and *Nfatc1-CreER* traces, showing that both populations contributed to the CA stem endothelium (Figure 2). Lineage-labeled cells from both Cre lines were regularly found in both the right and left CA stems. Thus, both progenitor cell types contribute to right and left CA stem formation, a reasonable outcome given the close apposition of the stem region to growing sinus venosus–derived coronary vessels and the endocardium.

VEGF-C is required for peritruncal vessel development. We next sought to identify the molecules involved in CA stem formation. Previous studies identified a role for VEGF-B in avian stem development (13), although, in mice, it appears to have a more prominent role in regulating cardiac vascularization and metabolism during injury rather than in development (29–32). To investigate whether other VEGF family members could have a role during mammalian coronary development, embryos were treated with the pan-VEGFR inhibitor axitinib in utero. This treatment could completely inhibit coronary vessel growth, identifying the VEGF pathway as a potential player during stem genesis (data not shown). Investigating the expression of different VEGF family members using *lacZ* knockin alleles revealed that VEGF-C was expressed in a pattern highly suggestive of a role in stem development. *Vegfc-lacZ* expression was detected within the walls of the outflow tract vessels and around their base (Figure 3, A–C). VEGF-C receptors were expressed in nearby cardiac endothelial cells. Peritruncal vessels (coronary vessels and ASVs) and the endocardium were positive for VEGFR2 and VEGFR3 (Figure 3D), while antibodies recognizing VEGFR2 also labeled aortic endothelium (Figure 3D). VEGF-A was also expressed in the heart, but it was largely expressed in cardiomyocytes throughout the ventricle (33) and not robustly expressed in the aortic wall or near its endothelium where stems normally form (Supplemental Figure 7). Thus, VEGF-C expression overlaps with the outflow tract and stem-forming regions (Figure 3C) and could signal to peritruncal and endocardial cells through VEGFR2 and VEGFR3.

Loss-of-function experiments were next performed to investigate the role of VEGF-C in CA stem formation. Depletion of VEGF-C had a dramatic effect. Although heart morphogenesis was grossly normal and other vessel beds were not affected (26), ASVs were completely missing and peritruncal coronary vessels were severely reduced in VEGF-C knockout animals (Figure 3E). Heterozygous animals exhibited an intermediate phenotype (Figure 3F). Many VEGF-C–deficient hearts did not have CA stems (Figure 3, G–I). Interestingly, in these knockout hearts, sprouts connected to the endocardium appeared to extend up toward the aorta (Figure 3G). When mutant animals did have stems, they were abnormally low on the aorta, connecting to the trough of the valve and pointing downward instead of to the side of the aorta above the aortic valvular sinus (Figure 3, H–J). This low positioning was closer to the deeper coronary vasculature that forms in knockout hearts. Data are shown for the right lateral side (right CA), but in most cases the left CA exhibited the same phenotype (Supplemental Figure 8A). These data indicate that VEGF-C is required for normal CA stem development due to its role in stimulating the first step of the process: the establishment of peritruncal vessels. In the absence of this growth factor, anomalous compensatory stems arise, possibly through interactions with endocardial sprouts.

Cardiomyocytes specifically populate the aortic wall where they are associated with developing CA stems. The knockout analysis and expression data described above show that VEGF-C is necessary for proper CA stem formation but that it does not pattern the precise connection site on the aorta. More specifically, VEGF-C is a powerful inducer of peritruncal vessel growth, but its expression extends into areas in which endothelial cells are not found, including the pulmonary artery and the vessel-free zone that surrounds the outflow vessels (Figure 1C and Figure 3, A–C). These observations suggest that other factors collaborate with VEGF-C–induced vessel growth to specify stem sites on the aorta. To identify candidate mechanisms, we looked for differences between the aorta and pulmonary artery by examining the spatial distribution of different cell types present at the relevant developmental stages. Our analysis included neural crest cells,

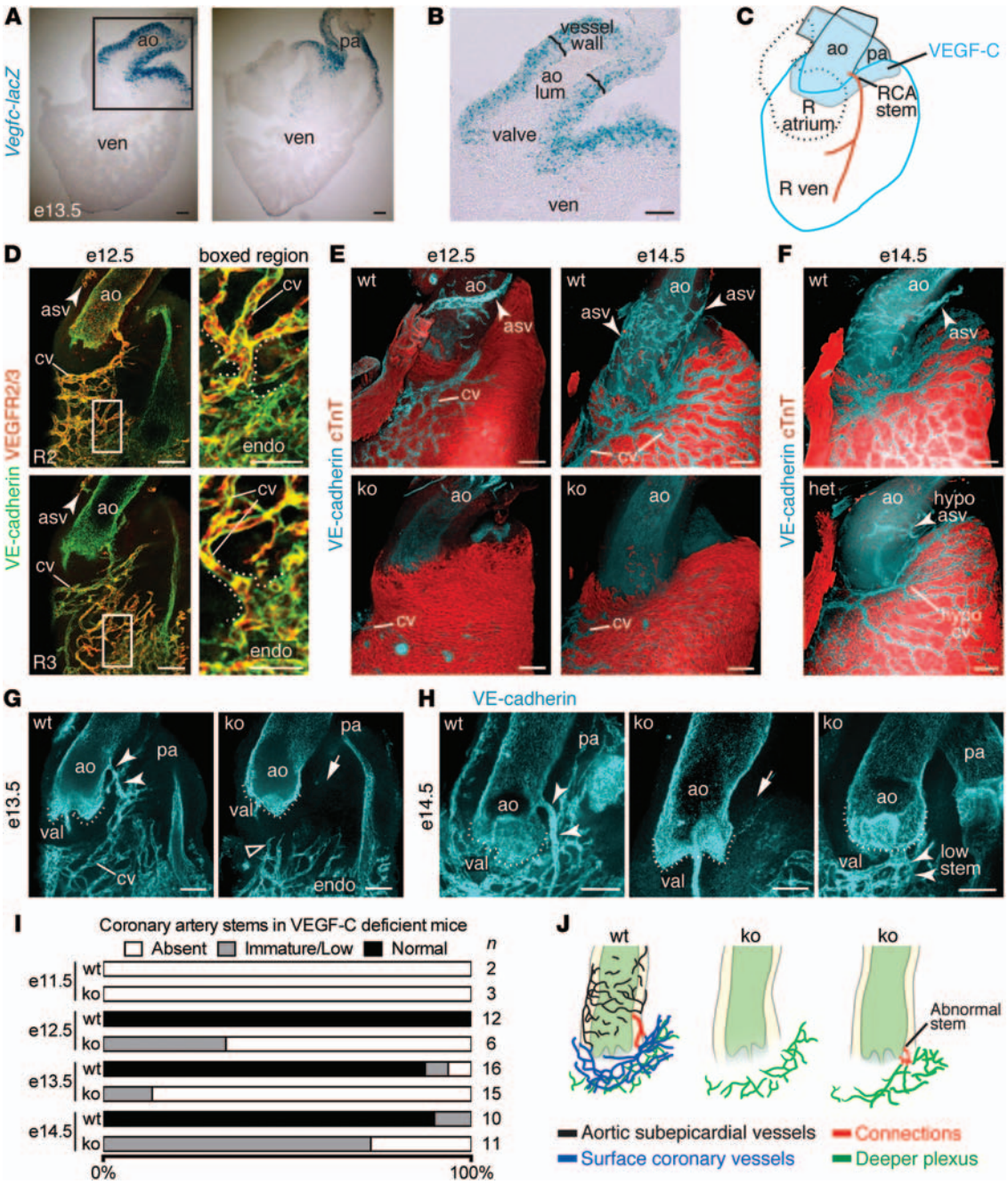

Figure 3. VEGF-C is required for peritruncal vessel growth and CA stem formation and patterning. (**A**) Tissue sections through *Vegfc–lacZ* hearts showing expression (blue) in the aorta and pulmonary artery. (**B**) Boxed region in **A** showing expression throughout the vessel wall (brackets) and base of the outflow tract. (**C**) Schematic of VEGF-C expression (blue). (**D**) VEGFR2 is expressed in all cardiac endothelial cell types while VEGFR3 is expressed in coronary and ASV endothelium and in the endocardium (endo). Right panels are high-magnification views of the boxed regions and show expression in coronary vessels that share cell-cell junctions with endocardial cells (dotted lines). (**E**) Confocal images showing the absence of peritruncal vessels (VE-cadherin$^+$, blue) around the outflow tract in VEGF-C–deficient hearts at E12.5 and E14.5. Cardiomyocytes are shown in red (cTnT). (**F**) Heterozygous (het) hearts have hypoplastic (hypo) peritruncal vessels. (**G** and **H**) CA stems (arrowheads) are present in wild-type but absent (arrows) or abnormal (arrowheads) in knockout (ko) hearts. The trough of each aortic valve sinus is traced with a dotted line for reference in comparison of stem location. (**G**) In many of the mutant hearts, sprouts connected to the endocardium (open arrowhead) appear to be extending up toward the aorta, even when other peritruncal vessels are absent. (**I**) Distribution of CA stem phenotypes in VEGF-C knockout embryos. *n* values are shown on the right. (**J**) Schematics of representative CA stems in VEGF-C–deficient outflow tracts. ao lum, aortic lumen; val, valve; ven, ventricle. Scale bars: 100 μm (**A**, **B**, left panel in **D**, and **E**–**H**); 50 μm (right panel in **D**).

smooth muscle cells, neurons, macrophages, epicardial cells, and cardiomyocytes. Of these, cardiomyocytes were the only cell type displaying an aorta-specific localization, suggesting a possible role in CA stem patterning.

Whole-mount imaging of E13.5 hearts showed that cardiomyocytes were abundant within the wall of the aorta but not in the pulmonary artery, in which they formed a sharp border at the level of the valve (Figure 4A). When this parameter was measured

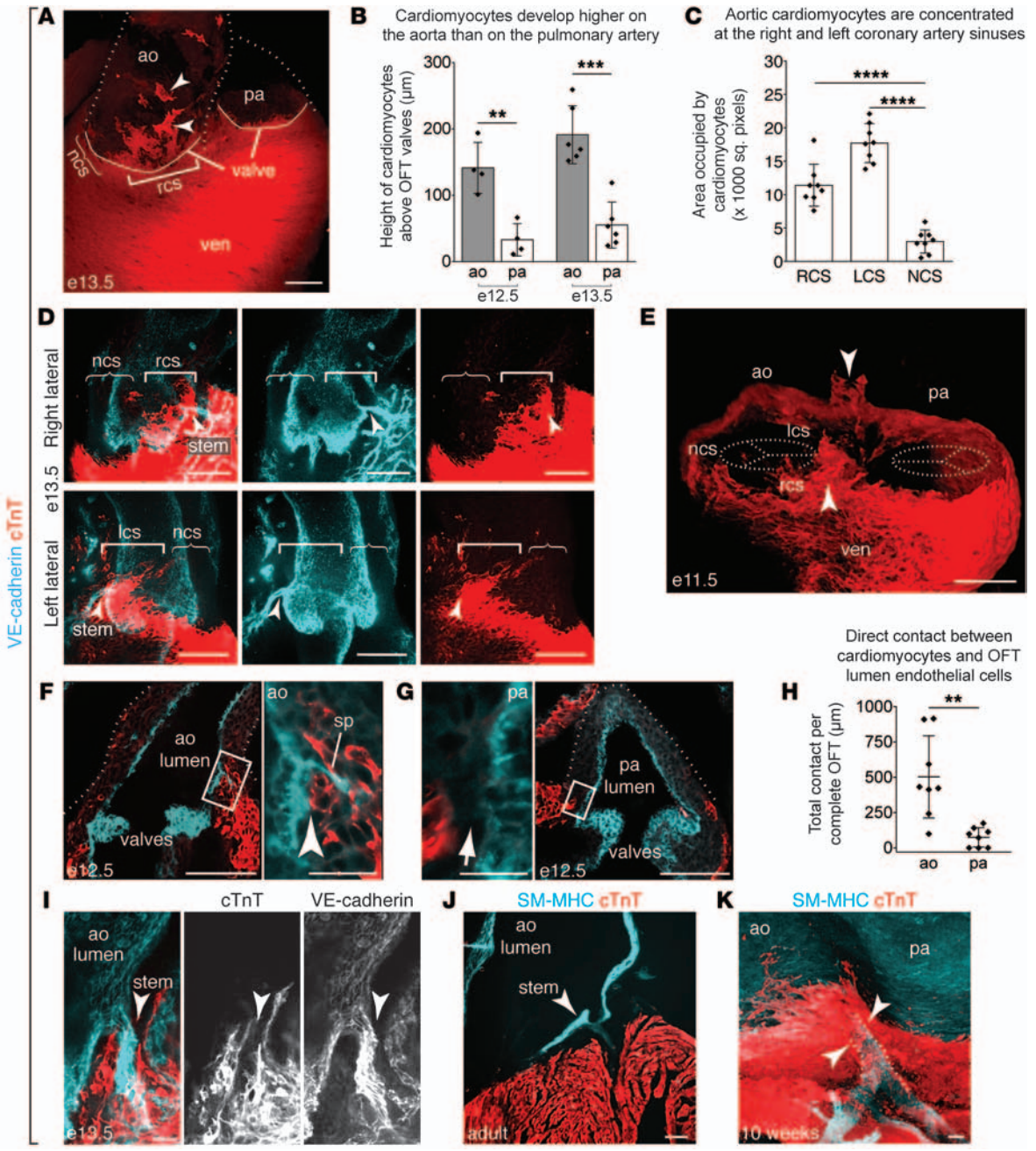

Figure 4. Aorta-specific cardiomyocyte development precedes CA stem formation. (**A**) Confocal image of the right lateral side of an E13.5 heart showing that cardiomyocytes (red, arrowheads) develop on the aorta distal to the valves but are absent in the analogous region of the pulmonary artery. The right coronary sinus (rcs) and noncoronary sinus (ncs) regions are indicated by square and curly brackets, respectively. (**B**) Quantification of cardiomyocytes within the aorta and pulmonary artery. (**C**) Quantification of cardiomyocytes among the different regions of the aorta. (**D**) Right and left lateral views of the aorta showing concentration of cardiomyocytes specifically around the right and left coronary sinuses (lcs) at the maturing stem sites (arrowheads). (**E**) Cardiomyocytes (arrowheads) are present in the aortic wall around the right and left coronary sinuses at E11.5 before stem formation. Aortic and pulmonary valve sinuses are schematized with dotted lines. (**F**) Cardiomyocytes directly contact the aortic endothelium (arrowhead) where aortic sprouts (sp) form – (**G**) but not the pulmonary artery (arrow), which never sprouts – as quantified in **H**. High-magnification views of the boxed regions are shown. (**I**) Developing CA stems (arrowhead) are closely associated with aortic cardiomyocytes. (**J**) Aortic cardiomyocytes are no longer present in adult hearts. (**K**) Developing human CA stems (arrowheads, dotted lines) are associated with aortic cardiomyocytes. OFT, outflow tract. All data represent mean ± SD. Each dot represents a value obtained from one sample. ****$P < 0.0001$; ***$P = 0.0001$ to 0.001; **$P = 0.001$ to 0.01. Scale bars: 100 μm (**A**, **D**, **E**, left panel in **F**, right panel in **G**, **J**, and **K**); 25 μm (right panel in **F** and left panel in **G**); 50 μm (**I**).

in tissue sections, cardiomyocytes were found to be significantly more distal from the valve in the aorta than in the pulmonary artery (Figure 4B). Measuring cardiomyocytes around the circumference of the aorta showed that they are significantly more concentrated at the left and right coronary sinuses when compared with the noncoronary sinus (Figure 4, C–E). The presence of aortic cardiomyocytes preceded stem formation, with aortic cardiomyocytes first observed at E11.5 (Figure 4E). At this time,

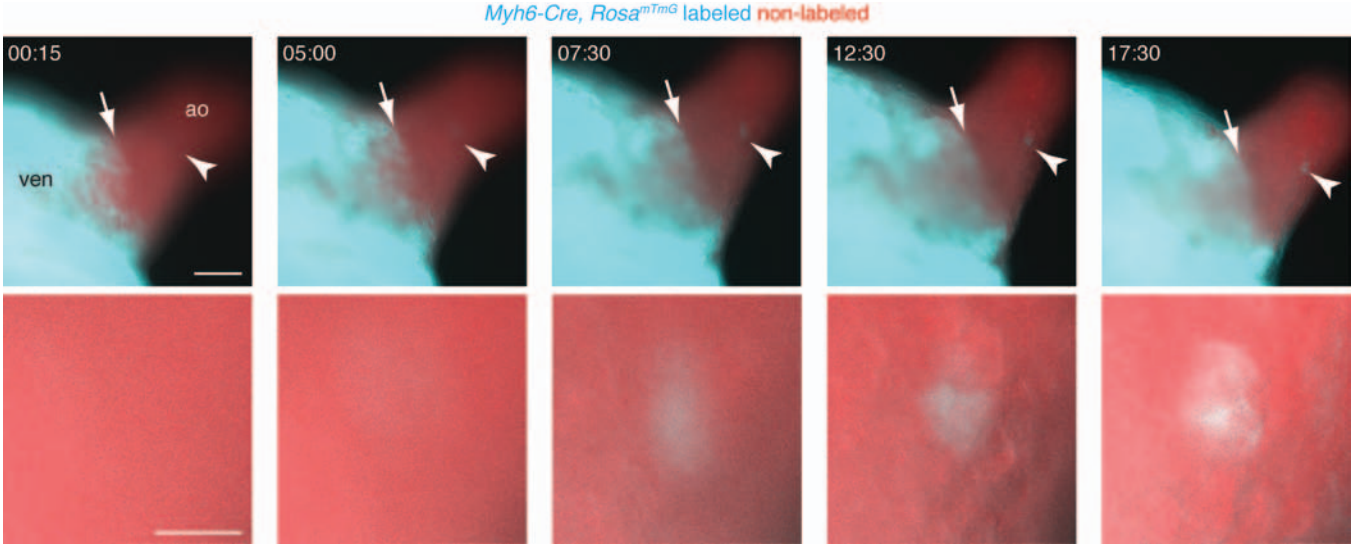

Figure 5. Aortic cardiomyocytes do not migrate up from the ventricle but differentiate in situ during explant culture. Images taken from time-lapse movies of E12.5 *Myh6-Cre, Rosa*^{mTmG} heart cultures. Cardiomyocyte migration is not observed (arrows) at the junction of the ventricle and aorta. Instead, there is the appearance of a new cardiomyocyte (arrowheads), which seems to have differentiated in situ (images are shown at higher magnification in bottom panels). Scale bars: 100 μm (top panels); 20 μm (bottom panels).

they were in direct contact with luminal endothelial sprouts from the aorta (Figure 4F). In contrast, cardiomyocytes were mostly separated from the pulmonary artery endothelium where sprouting was never seen (Figure 4G). Sectioning through the entire outflow tract and using serial sections to quantify the total amount of contact between cardiomyocytes and luminal endothelium revealed that there are significantly more direct interactions with the aorta compared with the pulmonary artery (Figure 4H). Thus, cardiomyocytes are present at the correct location and appropriate developmental stage to pattern CA stem formation.

We next observed the relationship between aortic cardiomyocytes and developing CA stems. Both the right and left stems were always closely associated with aortic cardiomyocytes in embryonic hearts (Figure 4I and Supplemental Figure 9, A and B). However, these cardiomyocytes disappeared postnatally, and stems were surrounded instead by smooth muscle (Figure 4J). A similar association between aortic cardiomyocytes and CA stems was seen during human embryogenesis (Figure 4K). This was particularly notable, since human CAs, unlike rodent CAs, are located on top of ventricular myocardium. We observed that human CAs connect with the aorta through a layer of aortic cardiomyocytes before they localize to the heart surface (Figure 4K). Thus, cardiomyocytes could play an important role in guiding CA stem development in mouse and human hearts.

Understanding how aortic cardiomyocytes arise on the aorta could be useful in devising loss-of-function experiments that test their role in stem formation. There are at least 2 routes by which cardiomyocytes could localize to the aorta: by migrating up from the ventricle or by directly differentiating from progenitor cells present in the aortic wall. The latter would be analogous to the mechanism of early heart growth, in which there are cardiomyocyte progenitors at the outflow and inflow poles that continuously differentiate and add to the heart tube (34, 35). To investigate these possibilities, we performed time-lapse microscopy on isolated hearts with fluorescently labeled cardiomyocytes (*Myh6-Cre, Rosa*^{mTmG}). While labeled cells could be seen proliferating, they never appeared to migrate (Figure 5). Instead, we frequently observed the initiation and gradual increase in cardiomyocyte-specific GFP expression on the aorta distal to the main ventricle, suggesting de novo differentiation ($n = 7$ hearts). This was in contrast to control experiments in which fluorescently labeled endothelial cells (*VE-cadherin-CreER, Rosa*^{tdTomato}) migrated rapidly while continuously extending and retracting filopodia (data not shown). These data suggest that aortic cardiomyocytes differentiate in situ and that inhibiting progenitor populations could decrease their presence.

Isl1 heterozygous hearts exhibit decreased aortic cardiomyocytes and abnormally low CA stems. Deletion of the transcription factor *Isl1* causes embryonic lethality and cardiac developmental defects (36). Without *Isl1*, cardiomyocyte progenitors in the second heart field fail to expand and contribute to heart growth, resulting in the lack of later developing structures, such as the right ventricle and outflow tract. We crossed the *Mef2c-AHF-Cre* mouse (37) to a *Rosa*^{mTmG} Cre reporter to lineage trace the second heart field and found that aortic cardiomyocytes descend from this cell population (Figure 6A). Since aortic cardiomyocytes arise from the second heart field lineage and appear to develop de novo from progenitor cells within the outflow tract, we tested whether deletion of one *Isl1* allele would affect their cell numbers in the aorta. Observing cardiomyocytes using whole-mount confocal micrographs of wild-type and *Isl1* heterozygous hearts revealed a reduction of this cell type in the aortic wall at both the right and left CA stem regions (Figure 6, B and C, and Supplemental Figure 8B). Measuring the presence of cardiomyocytes distal to the valves via optical sections showed a significant decrease in the cardiomyocyte distribution in mutant embryos (Figure 6D). We did not find any gross defects in heart morphogenesis, as outflow tract rotation was normal (Figure 6B) and myocardial thickness and total heart size were similar in wild-type littermates (Supplemental Figure 10). The amount of smooth muscle around the aorta near the stem site was not seri-

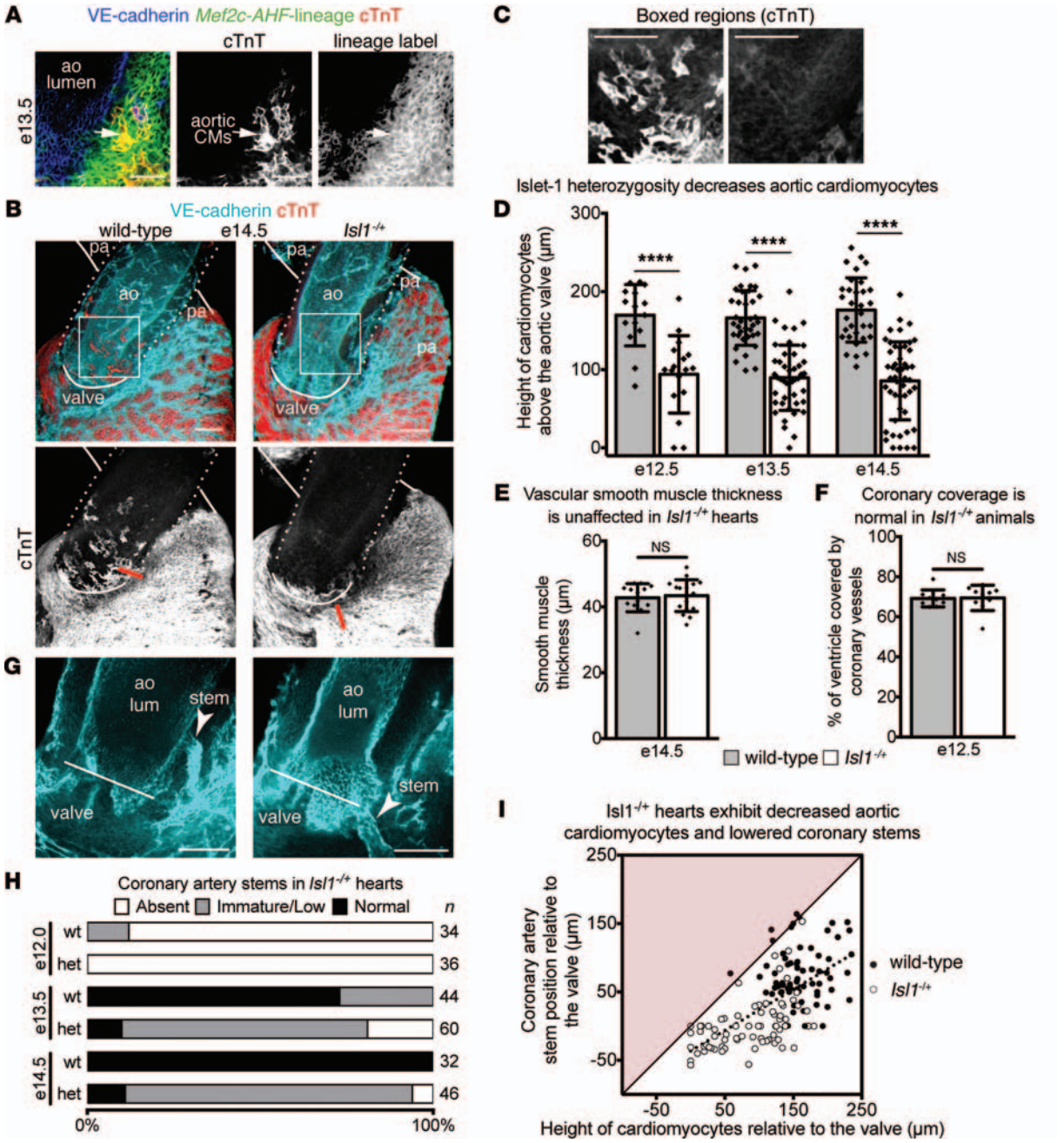

Figure 6. ISL1 heterozygosity decreases aortic cardiomyocytes and disrupts normal stem development and positioning. (**A**) Second heart field lineage tracing (*Mef2c-AHF-Cre, Rosa*^{mTmG}) labels aortic cardiomyocytes (CMs, arrows). (**B**) Confocal images of wild-type and *Isl1* heterozygous embryos showing decreased numbers of cardiomyocytes within the aorta (dotted line). The pulmonary artery is also outlined (solid lines). Cardiomyocytes (cTnT$^+$) are shown in red; peritruncal vessels (VE-cadherin$^+$) are shown in blue. The bottom panel shows only the cTnT channel where red lines indicate the stem position. (**C**) Boxed regions in **A** showing only the cTnT channel. (**D**) Quantification of the length distal to the valve occupied by aortic cardiomyocytes shows a significant decrease in *Isl1* mutant hearts. (**E** and **F**) Other developmental parameters, (**E**) smooth muscle cell development and (**F**) coronary vessel growth, are unchanged in mutant hearts. (**D**–**F**) Data represent mean ± SD. Each dot represents a value obtained from one sample. (**G**) *Isl1* heterozygous hearts have abnormally low stem positioning with respect to the valves (lines) in comparison to wild-type hearts. (**H**) Distribution of stem phenotypes observed in *Isl1* mutant and wild-type hearts. *n* values are shown on the right. (**I**) The height of CA stems does not significantly rise above the level of aortic cardiomyocytes in both wild-type and mutant hearts, as evidenced by the paucity of points in the pink area ($y > x$) of the graph. These data were measured at E14.5. A linear regression for the data set (dotted line, $y = 0.5999x - 36.39$) indicates a positive correlation. ****$P < 0.0001$; NS ≥ 0.05. Scale bars: 100 μm.

ously affected (Figure 6E), and there were no obvious abnormalities in other cell types such as neurons (data not shown). *Isl1* mutation did not produce a general vessel growth defect, since coronary sprouting over the ventricles in heterozygous mice was normal (Figure 6, B and F). Although we cannot rule out differences in cell types or functions not analyzed, *Isl1* heterozygous mice appear to have a relatively well-isolated defect in aortic cardiomyocytes, making them useful in testing the role of these cells in CA stem formation.

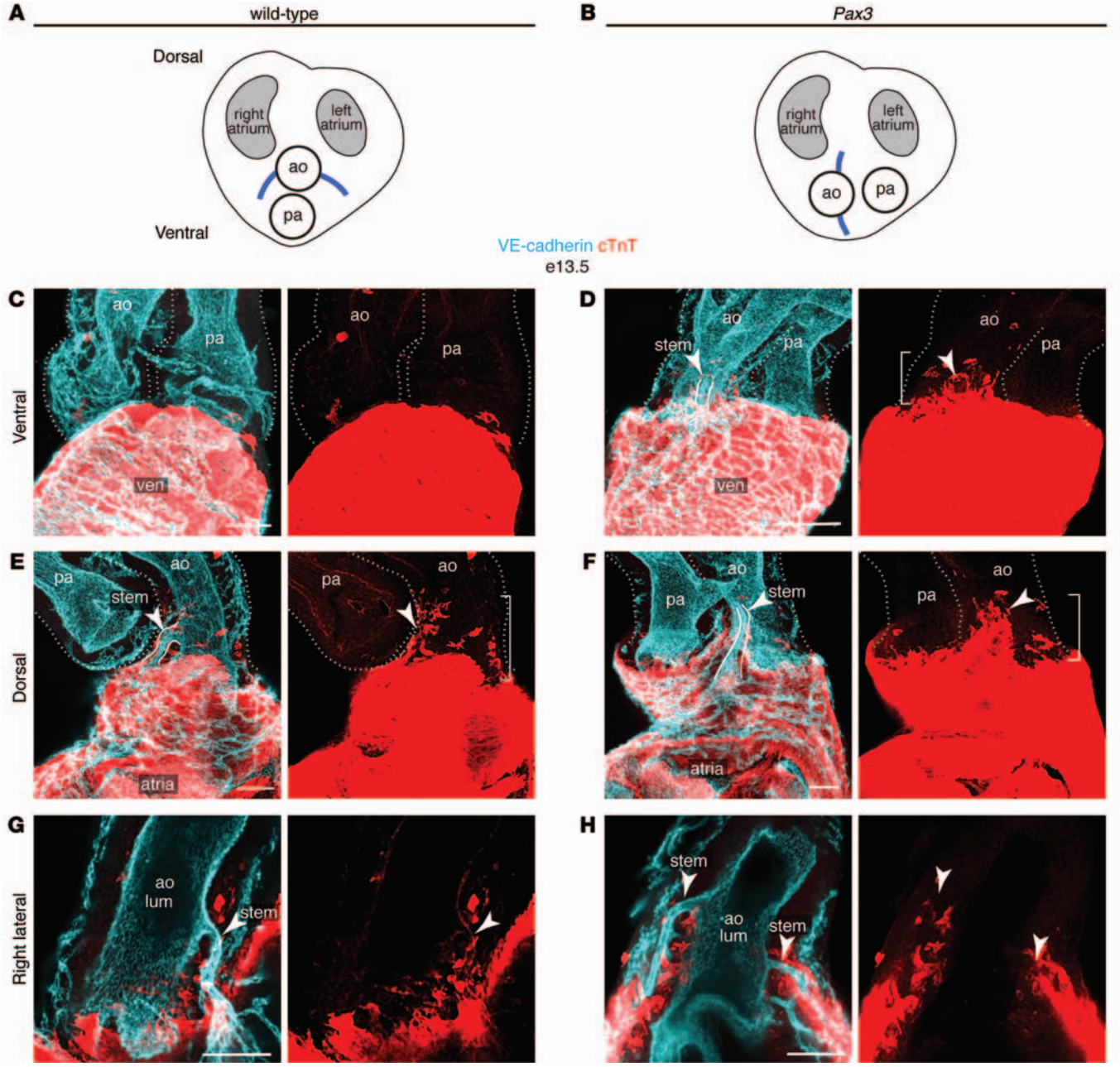

Figure 7. Misplaced CA stems are correlated with aortic cardiomyocytes in hearts from *Pax3*-null embryos. (**A** and **B**) The side-by-side positioning of the aorta and pulmonary artery in hearts from (**B**) *Pax3*-null embryos compared with (**A**) wild-type embryos. Blue lines indicate the locations of CA stems. (**C**–**H**) Confocal images of hearts immunofluorescently labeled for VE-cadherin (endothelium) and cTnT (cardiomyocytes). CA stems (arrowheads) associate with aortic cardiomyocytes (brackets) in wild-type and in *Pax3* knockouts. CA stems are outlined in solid lines in **D**–**F**. Outflow tracts are outlined with dotted lines in **C**–**F**. Images in **G** and **H** are maximum projections of optical sections through the aortic lumen captured from the right lateral side of the heart. Scale bars: 100 μm.

CA stems in *Isl1* mice were dramatically different than those in wild-type mice. Stems attached much lower on the aorta, often localizing to the trough of the valve (Figure 6G and Supplemental Figure 6, A and B). In addition, initial connections between peritruncal vessels and the aorta were frequently delayed (Figure 6H). This phenotype was seen in both the right and the left CA stems (Figure 6 and Supplemental Figure 8C). Stem sites were quantified by drawing a line at the top of the valves where the leaflets converge and measuring the distance from this line to where the stem connects to the aorta (Figure 6G and Supplemental Figure 6, A and B). Positive values indicate the stem orifice was above (distal to) the valve. Negative values indicate the stem orifice was below the valve. A value of 0 was assigned to a stem that connects at the exact level of the valve. Plotting this location against the region occupied by cardiomyocytes revealed a positive correlation between the 2 parameters (Figure 6I). This analysis highlighted that stems did not attach above the region where cardiomyocytes were found (i.e., no data points were significantly above the line $y = x$), even in *Isl1* mutants with dramatically lowered aortic cardiomyocytes (Figure 6I). These data support a

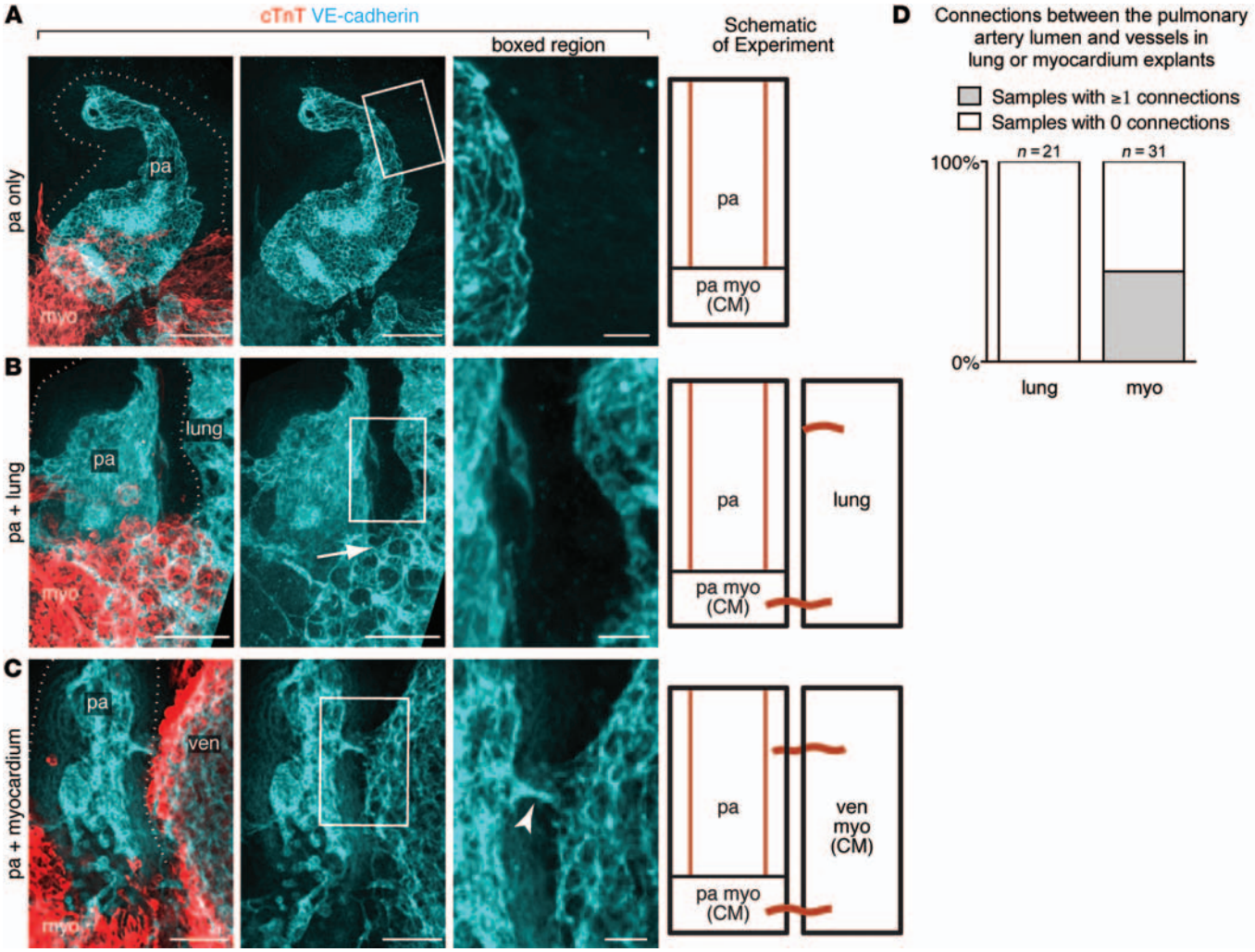

Figure 8. Ectopic vessel connections with the pulmonary artery lumen can form in the presence of cardiomyocytes. (**A**–**C**) Confocal images of pulmonary artery outflow tract explants cultured alone or adjacent to other tissues. Endothelial cells are labeled in blue (VE-cadherin$^+$), and cardiomyocytes are labeled in red (cTnT$^+$). Schematics summarizing experimental setup and results are shown. (**A**) Pulmonary artery explants retain a luminal endothelial layer that does not sprout into the vessel-free zone (dotted line). (**B**) Endothelial cells within lung tissue do not connect with the pulmonary artery lumen but do migrate into the myocardial (myo) region at its base (arrow), which contains cardiomyocytes. (**C**) When cardiomyocytes from ventricular myocardium (ven myo) are placed alongside artery explants, ventricular coronary vessels frequently form connections (arrowhead) with the pulmonary artery endothelium. (**D**) Percentage of explant samples that did or did not form connections with the pulmonary artery lumen when cultured beside lung or ventricular myocardium. Scale bars: 100 μm (left and center panels in **A**–**C**); 25 μm (right panels in **A**–**C**).

model in which cardiomyocytes within the aortic wall guide the formation of CA stems at their proper location on the lateral sides of the aorta just distal to the valves.

Misplaced CA stems associate with aortic cardiomyocytes in hearts with outflow tract rotation defects. During heart development, the outflow tract undergoes a rotation event as it is transformed from a single vessel into the aorta and pulmonary artery. This process positions the aorta between the atria and pulmonary artery (Figure 7A). TGA is a congenital heart defect that is a consequence of insufficient rotation, causing the aorta and pulmonary artery to be reversed or side by side (Figure 7B). This malformation is also associated with variations in CA stem placement (Figure 7B). We used *Pax3*-null mice (38), which have defective neural crest cell migration that frequently leads to TGA, to examine whether malrotation affects aortic cardiomyocyte growth and whether these cells still associate with CA stems under abnormal conditions.

Analyzing *Pax3* mutants that exhibit TGA (outflow tract septation without proper rotation) revealed that neither normal neural crest migration nor complete rotation was required for aorta-specific cardiomyocyte growth (Figure 7, C–H). Although the aorta and pulmonary artery were side by side in mutant hearts, cardiomyocytes were specifically present in large numbers on the aorta (Figure 7, D and F). Mutant hearts also had coronary vessels that exited the aorta ventrally (from the front) and dorsally (from the back) instead of laterally, from the right and left sides (Figure 7, A and B). However, the misplaced CA stems were always associated with a concentration of cardiomyocytes growing within the aortic wall (Figure 7, D, F, and H) ($n = 12$ hearts). These data provide further evidence of a developmental relationship between cardiomyocytes and CA stems.

Cardiomyocytes can induce ectopic connections with the pulmonary artery in vitro. We next performed gain-of-function experiments to investigate whether cardiomyocytes could induce vas-

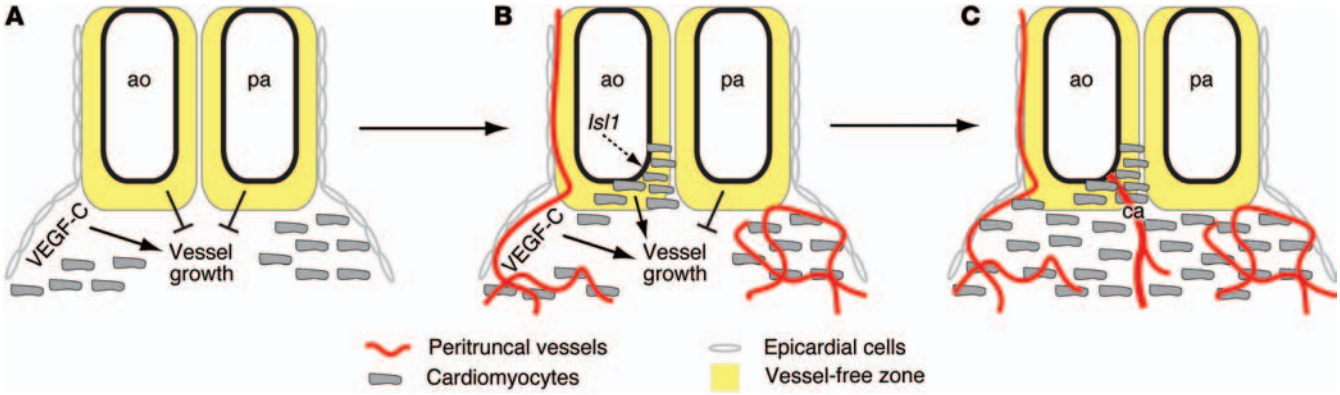

Figure 9. Proposed model for the role of VEGF-C and aortic cardiomyocytes in CA stem formation. (**A**) VEGF-C stimulates vascular growth near the outflow tract, while a vessel-free zone directly surrounds the aorta and pulmonary artery. (**B**) Peritruncal vessels develop around the outflow tract but do not invade the vessel-free zone. Wild-type *Isl1* expression levels in the embryo allow cardiomyocytes to differentiate specifically in the aortic wall where they support vessel growth and facilitate connections between peritruncal vessels and lumen endothelium. (**C**) The result is a correctly positioned CA stem (ca) on the aorta.

cular connections where they normally do not occur. Outflow tract explants were cultured adjacent to ventricular myocardium or control tissues. After 2 to 3 days, the explants were immunostained to determine whether ectopic vascular connections occurred specifically in the presence of cardiomyocytes. When cultured alone, explanted pulmonary arteries maintained their general shape, with a nonsprouting luminal endothelial layer surrounded by a vessel-free region (Figure 8A). Endothelial cells from lung explants did not invade the vessel-free region, even though they readily migrated into the myocardium at the base of the artery explant (Figure 8, B and D). In contrast, culturing myocardium adjacent to outflow tracts frequently resulted in connections between ventricular coronary vessels and pulmonary artery luminal endothelium (Figure 8, C and D). Thus, myocardium can mediate ectopic connections between the pulmonary artery and the coronary vessels in vitro, supporting the hypothesis that aortic cardiomyocytes facilitate this process during stem development.

Discussion

In this study, we describe 2 morphological steps that are required for CA stem patterning — (a) the establishment of the peritruncal vessels that surround the aorta and (b) anastomosis of these vessels specifically with the aorta — and provide insight into the molecular and cellular mechanisms guiding both processes. Our data show that VEGF-C mediates step one. It is highly expressed throughout the outflow tract, and VEGF-C–deficient mice have absent ASVs and hypoplastic peritruncal coronary vessels. Step one is required for CA stem patterning, as evidenced by the delayed, misplaced stems that form in VEGF-C mutant hearts when the peritruncal vessels are reduced or missing. VEGF-C is expressed throughout the outflow tract, including regions in which endothelial cells do not grow, suggesting that it alone is not sufficient for stimulating connections with the aorta at defined locations. We found that cardiomyocytes are localized in a pattern suggestive of a role in step two. They are concentrated along the wall of the aorta in which stems form but are mostly absent from the pulmonary artery. *Isl1* heterozygosity decreases aortic cardiomyocytes and results in delayed, abnormally placed stems. Misplaced stems on hearts with outflow tract rotation defects formed within regionally shifted aortic cardiomyocytes, and cardiomyocytes induced ectopic connections with the pulmonary artery in culture. These data support a step-wise model in which peritruncal vessels are attracted to the outflow tract from nearby vessel beds (the sinus venosus, endocardium, and surface of the aorta) in response to VEGF-C, after which cardiomyocytes facilitate the positioning of their fusion sites on the aorta (Figure 9). Failure to complete either step results in abnormal CA stem patterning.

CA anomalies in humans can range from nonstandard stem origin on the aorta to defects in which the left coronary stem branches from the pulmonary artery (ALCAPA). Anomalous origins on the aorta have been estimated to occur in approximately 1% of the population (1). These are frequently asymptomatic but can cause myocardial ischemia and sudden cardiac death in a significant number of cases (2, 39). Anomalous CA stems can attach to the aorta in a number of different configurations, which may explain the spectrum of symptoms. The most clinically concerning anomalies for sudden cardiac death occur when the artery stem attaches to the opposite aortic sinus, which causes the vessel to travel between the aorta and pulmonary artery, e.g., the left CA arising from the right sinus. The direct cause of ventricular ischemia in these cases is not known but is thought to arise when the aorta and pulmonary artery apply pressure to the intervening CA, obstructing the vessel lumen. Understanding how to handle CA anomalies is particularly important for athletes and military recruits preparing to undergo intense training. CA anomalies are estimated to be responsible for 17% of sudden cardiac deaths in young competitive athletes (40). An American Armed Forces Institute of Pathology study found that 33% of cardiac-related deaths in new recruits undergoing training were associated with anomalous left CAs arising from the right coronary sinus (41). Specialists in the field are focused on developing imaging techniques for accurate screening and devising prophylactic strategies following diagnosis (42).

The condition in which coronary arteries connect to the pulmonary artery (ALCAPA) is a much more serious and life-threatening anomaly than instances of nonstandard stem placement on the aorta. ALCAPA has been calculated to occur in 1 in 300,000 births, and approximately 90% of patients with this condition do not survive past infancy without surgical repair (43, 44). Those who

do survive develop extensive, disorganized compensatory vasculature around the heart and are at increased risk for severe coronary complications in adulthood. Interestingly, unlike many congenital cardiac malformations, ALCAPA is usually an isolated defect observed in the absence of other abnormal structural changes, though an underlying genetic cause for this condition has not yet been identified. Our data suggest that *Vegfc* or *Isl1* mutations could be possible candidates. A better understanding of the developmental and potential genetic basis of this syndrome could lead to less invasive, alternative interventions for ALCAPA.

VEGF receptor signaling is an important regulator of coronary vessel development, but a site-specific role of individual family members has not been delineated for stem development. Cardiomyocytes within the main ventricle produce VEGF-A (33, 45), and coronary vascular development is decreased when VEGF-A is inhibited (13, 46, 47). Specific deletion of this factor from cardiac cells primarily affects the microvasculature (48) and coronary vessels within the myocardium (27). VEGF-A expression is downstream of a signaling cascade in which FGFs induce sonic hedgehog to regulate coronary development (49, 50). VEGF-A also has an important role in myocardial and valve development. With VEGF-A inhibition or deletion, the myocardial layer is thin, containing fewer cardiomyocytes (13, 27, 48). The developing valves require a complex temporal sequence of VEGF signaling, involving first VEGFR1 and then VEGFR2, to carry out the process of cushion formation and subsequent maturation (51–53). Thus, VEGF-A is multifunctional during heart development, possibly complicating interpretations of its role in coronary vascularization, which is thought to be dependent on hypoxic signals triggered within the expanding myocardium (54).

Our data indicate that VEGF-C has a more specific function during cardiac development, even within the coronary vasculature. Myocardial thickness and valve structure are not perturbed in knockout hearts, which is consistent with the more restricted expression pattern of VEGF-C in the outflow tract vessels and epicardium (26). In another study, we showed that VEGF-C deletion specifically affects sinus venosus–derived coronary development but not coronary vascularization from other sources on the ventral side of the heart and septum (likely from the endocardium, refs. 25, 27, or proepicardium, ref. 28) (26). This specific effect is unsurprising, given that sinus venosus sprouting is initiated directly beneath the epicardium (which expresses VEGF-C), while ventral sprouting is first seen deeper within the myocardium (which expresses VEGF-A) (25–27). VEGF-C expression in the outflow tract is required for the first step in CA stem development. Few peritruncal vessels develop in the absence of VEGF-C, precluding their connections with the aorta. In knockout hearts, endothelial projections that are connected to endocardium can be seen sprouting toward the outflow tract. We hypothesize that these vessels give rise to the delayed, abnormally low stems that were seen in some of the mutants. Indeed, *Nfatc1-CreER* lineage tracing experiments show that endocardial-derived coronary vessels contribute to CA stems. The formation of these lowered stems could involve endocardial activation in response to VEGF-A expressed by ventricular cardiomyocytes. In summary, VEGF-C is important for CA stem patterning, because, in the absence of peritruncal vessels, stems form in abnormal locations.

Our results identified cardiomyocytes as a cellular feature specific to the aorta. Cardiomyocytes are known to foster vascular growth by secreting angiogenic molecules (23, 24, 55), supporting the hypothesis that they facilitate the establishment of stems at the correct location. However, preliminary experiments deleting *Vegfa* using various cardiac Cre lines did not suggest a role for this growth factor. Future experiments will focus on identifying the specific cardiomyocyte-derived molecule mediating stem positioning. An additional possibility is that these cells are antagonizing an antiangiogenic factor present in the walls of the outflow tract. Indeed, large arteries are frequently surrounded by an avascular zone, as is the case with the developing aorta and pulmonary artery. In our experiments, endothelial cells did not migrate into the region surrounding outflow tract explants (unless cardiomyocytes were present), suggesting the existence of antiangiogenic factors. Precedent for such a mechanism is seen with the extracellular matrix protein chondromodulin-1, which restricts vessel growth in the cardiac valves during development and in the adult (56). Similarly, the vessel-free zone around the outflow arteries expresses numerous extracellular matrix molecules, which, in other systems, have been shown to liberate antiangiogenic peptides following proteolytic processing (57).

The mechanisms by which cardiomyocytes specifically populate the aortic wall are actively under investigation. Aortic cardiomyocyte development is disrupted by heterozygosity for the transcription factor *Isl1*. This transcription factor marks the second heart field, which contributes to heart growth, by adding cells onto the early heart tube to produce the outflow tract, right ventricle, and atria (58). Functionally, *Isl1* supports cardiomyocyte progenitor proliferation, causing *Isl1*-null animals to lack the majority of second heart field–derived cardiac structures (36). In fact, we found that aortic cardiomyocytes derive from the second heart field. These observations suggest that aortic cardiomyocytes may develop via mechanisms analogous to those of second heart field maturation but in an aorta-specific manner. There may be an aorta-specific delay in the differentiation of second heart field progenitors in response to molecules specifically expressed in this outflow vessel. There are genetic distinctions between the aorta and pulmonary artery. The base of the pulmonary artery specifically expresses a *Myf5* promoter fragment (*96-16* transgene) (59) and *Sema3c* (18), while the corresponding region on the aorta expresses an *Fgf10* fragment (*T55* transgene) (18). Ultimately, insight into the embryonic mechanisms that trigger CA stem development on the aorta could be commandeered to establish new vessels in the adult as treatments for congenital cardiac defects and coronary heart disease.

Methods

Animals

The following mouse strains were used: wild-type (CD1, Charles River Laboratories), *Apj-CreER* (see below), *Vegfc-lacZ* (provided by K. Alitalo, University of Helsinki; ref. 60), *Vegfa-lacZ* (provided by L. Miquerol, Aix Marseille Université, Developmental Biology Institute of Marseille, Marseille, France; A. Damert, Babes Bolyai University, Cluj-Napoca, Romania; and A. Nagy, Lunenfeld-Tanenbaum Research Institute, Toronto, Ontario, Canada; ref. 33), *Vegfc*^{fl} (provided by K.

Alitalo and P. Saharinen, University of Helsinki; see below), *Isl1*^{MerCreMer} (provided by S. Evans, University of California, San Diego, La Jolla, California, USA; ref. 61), *Rosa*^{mTmG} Cre reporter (The Jackson Laboratory, *Gt(ROSA)26Sor*$^{tm4(ACTBtdTomato,EGFP)Luo/J}$), *Rosa*^{tdTomato} Cre reporter (The Jackson Laboratory, *B6.CgGt(ROSA)26Sor*$^{tm9(CAGtdTomato)Hze/J}$), *Pax3* (The Jackson Laboratory, *Pax3*$^{tm1(cre)Joe/J}$), *B6.FVB-Tg(Myh6-cre)2182Mds*) (*Myh6-Cre*, The Jackson Laboratory, *Mef2c-AHF-Cre* (provided by B. Black, University of California, San Francisco, San Francisco, California, USA; ref. 37), *VE-cadherin-CreER* (provided by L. Iruela-Arispe, University of California, Los Angeles, Los Angeles, California, USA; ref. 62), *Nfatc1-CreER;Rosa26*$^{RFP/+}$ (provided by B. Zhou, Shanghai Institutes for Biological Sciences; ref. 63), and *Apelin-nlacZ* (provided by T. Quertermous, Stanford University; ref. 64). CD1 mice were used for wild-type characterization studies. In general, other mouse lines were maintained on a mixed background of C57BL/6J and FVB unless otherwise noted. *Vegfc* knockout and floxed mice were ICR. The floxed line was crossed to *Rosa-CreER* on a mixed C57BL/6J and 129SV background (described below). In all cases, wild-type littermate controls were compared with mutant animals. Among the mouse lines used, we did not detect evidence of any strain-dependent differences in early stem targeting.

The majority of VEGF-C–deficient embryos were produced by crossing a ubiquitously expressed, tamoxifen-inducible *Cre* line to a *Cre*-dependent (conditional) deletion allele. Mice with conditionally targeted *Vegfc* alleles were created by inserting the mouse *Vegfc* cDNA and a *Frt*-flanked *Neo* cassette in the first exon of the mouse *Vegfc* genomic locus, thereby deleting the first exon and part of the first intron of the mouse *Vegfc* gene. Additionally, the inserted *Vegfc* cDNA was flanked by *LoxP* sites. Heterozygous mice were mated with the *Flp* deletor mouse strain to remove the *Neo* cassette and were subsequently mated to homozygosity. The homozygous *Vegfc*$^{fl/fl}$ mice were viable, with no abnormal phenotype. Mating of the *Vegfc*$^{fl/fl}$ mice with the *R26R-Cre* mice resulted in efficient deletion of the gene and caused the expected embryonic lethality based on previous data from constitutive *Vegfc* knockout mice (60).

To create an *Apj-CreER* mouse line, recombineering (65, 66) was used to insert a *CreERT2* gene at the *Apj* start site of a BAC. The *Apj* BAC was procured from the Children's Hospital Oakland Research Institute and represents 153,553 base pairs of chromosomal DNA derived from a male C57BL/6J mouse (clone RP24-301A16, Children's Hospital Oakland Research Institute). Modified *Apj* BACs were injected into oocyte pronuclei (Cyagen Biosciences) that were transferred into pseudopregnant females. Resulting pups were screened for incorporation of BAC DNA, and 2 founder lines were established and found to exhibit similar expression patterns.

To generate embryos expressing Cre plus an allele of interest, a male parent containing the Cre gene (and the floxed allele, if applicable) was mated with a female parent containing either the Cre-inducible reporter or the floxed gene. This breeding scheme was performed to avoid floxing out genes in the female parent during pregnancy, minimizing potentially confounding variables in the resulting embryo phenotypes. For all breeding schemes, mice were between 2 and 6 months of age.

In some cases, mice were treated with tamoxifen to induce *CreER*-based recombination. *Apj-CreER* and *Nfatc1-CreER* lineage-tracing experiments were carried out by injecting pregnant dams intraperitoneally with 4 mg tamoxifen dissolved in corn oil. To obtain VEGF-C–deficient animals, the *Vegfc*^{fl} line was crossed to mice containing the *R26R-CreER* transgene, which expresses a tamoxifen-inducible Cre recombinase in most cells. To activate Cre expression, mice were given 100 μl 4-OH-tamoxifen (25 mg/ml) by oral gavage on E6.5 and E7.5 (prior to *Vegfc* expression).

For assessment of aortic sprouting in the absence of peritruncal vessels, coronary vessels and ASVs were completely inhibited with intraperitoneal injections of the VEGFR antagonist axitinib (Sigma-Aldrich) on E10.5 and E11.5 (25 mg/kg, 1 BID). Hearts were isolated at E12.5 and immunostained as described below.

Immunohistochemistry and imaging

To obtain staged embryos and hearts, timed pregnancies (morning plug designated E0.5) were dissected and fixed in 4% paraformaldehyde and stored in PBS. Fixed tissues were left intact or sectioned and then processed for either whole-mount or section immunofluorescence. Some tissues were subjected to an X-gal reaction. Immunofluorescence was performed in either 1.5-ml tubes (whole mount) or on microscope slides (tissue sections) using the same protocol, except the former was subjected to constant rotation. Primary antibodies were diluted in blocking solution (5% goat or donkey serum, 0.5% Triton X-100 in PBS) or in PBS with 0.5% Triton X-100 (PBT) and incubated with tissues overnight at 4°C. Tissues were then washed with PBT 3 times for 1 hour before another overnight incubation with secondary antibodies diluted in blocking solution or in PBT. Specimens were then washed again, placed in Vectashield (Vector Laboratories), and imaged using either an inverted Zeiss LSM-700 confocal microscope (whole-mount tissue) or Axioimager A2 epifluorescence microscope (tissue sections). Images were digitally captured and processed using ImageJ (NIH), Photoshop (Adobe Systems), Zen (Carl Zeiss), and AxioVision (Carl Zeiss) software packages. The following primary antibodies were used: VE-cadherin (BD Biosciences, 550548, 1:100); cTnT (Developmental Studies Hybridoma Bank, CT3-c, 1:500); SM-MHC (Biomedical Technologies, BT-562, 1:300); WT-1 (Abcam, ab15249, 1:100); CD31 (BD Biosciences, 550274, 1:100); PROX1 (R&D Systems, AF2727, 1:300), ERG-1/2/3 (Santa Cruz Biotechnology, C-20, 1:100); LYVE-1 (eBiosciences, 14-0443-80, 1:100); VEGFR2 (R&D Systems, AF644, 1:100); and VEGFR3 (R&D Systems, AF743, 1:100). Secondary antibodies were Alexa Fluor conjugates 488, 555, 594, 633, 635, and 647 (Life Technologies) used at 1:250. DAPI (Sigma-Aldrich, 1:2000) was also used.

Perfusion experiments

The patency of CA stems was assessed by injecting FITC-conjugated tomato lectin (Vector Laboratories) into the left ventricle of dissected embryos. The lectin was distributed throughout the vasculature via cardiac contraction. Tissue sections were prepared and imaged as described above, and vessels containing the fluorescent lectin were considered patent.

Organ cultures

For cocultures, dissected outflow vessels, ventricles, and lungs from E12.5 or 13.5 wild-type embryos were placed on 8-μm Millicell cell culture inserts (EMD Millipore) at the air-liquid interface. Cultures were maintained in DMEM media with 10% fetal bovine serum and 100 U ml^{-1} penicillin and 100 μg ml^{-1} streptomycin at 37°C/5% CO_2 for 48 to 72 hours and then fixed and subjected to whole-mount immunofluorescence as described above.

Time-lapse imaging of aortic cardiomyocytes and cardiac endothelial cells was performed using embryonic hearts from *Myh6Cre*, *Rosa*^{mTmG} and *VE-cadherin-CreER, Rosa*^{tdTomato} mice, respectively. As described above, hearts (with the atria and sinus venosi removed) were cultured with aortas facing upward. Images documenting their development were captured every 15 minutes for 20 hours by an inverted Zeiss Observer.Z1 microscope configured with a XL-3 stage incubation chamber (with temperature and CO_2 control) using AxioVision SE64 Rel. 4.9 software.

Quantification

Aortic cardiomyocyte and CA stem height. In wild-type hearts, the location of cardiomyocytes in the wall of the aorta and pulmonary artery was measured in sagittal tissue sections. For *Isl1* heterozygous and wild-type littermates, optical sections from confocal z-stacks imaged from the right lateral side were used to quantify the position of aortic cardiomyocytes and stems. In all cases, values were obtained by measuring the distance between the valvular endothelium where the leaflets converge and the distal-most cardiomyocyte or stem. CA stems at or below the level of the valve leaflet meeting point were considered "low," since this was rare for wild-type samples (Figure 6I and Supplemental Figure 6). AxioVision and Zen software packages from Zeiss were used to perform measurements in tissue and optical sections, respectively.

The area occupied by cardiomyocytes at the different aortic valve sinuses (left coronary, right coronary, and noncoronary) was measured by imaging entire aortas from the right and left lateral sides. Right lateral images were transferred into ImageJ, and the area above the troughs of the valves covered in cardiomyocytes was measured for the right coronary sinus and noncoronary sinus regions (see Figure 4D). A similar measurement was performed for the left lateral images. The noncoronary sinus values from the right and left views were summed while the right and left coronary sinus values were taken solely from the respective images. Values were reported as pixels (Figure 4C).

To quantify the total amount of contact between cardiomyocytes and outflow tract luminal endothelium, the length in which the 2 cell types were directly adjacent was measured in every serial section through the entire vessel. The values from every section were summed to determine the total contact for one individual aorta or pulmonary artery.

Myocardial and smooth muscle thickness. Myocardial and smooth muscle thickness were quantified using optical sections from confocal z-stacks of hearts immunolabeled for cTnT and SM-MHC, respectively. Myocardial measurements were taken from sagittal views through the dorsal wall of the right ventricle. Smooth muscle thickness measurements were taken from sagittal views through the ventral wall of the aorta. All measurements were performed using Zeiss Zen software.

Heart size and coronary vessel growth. Total heart size and coronary vessel growth was measured for *Isl1* heterozygous and wild-type hearts at E12.5 using ImageJ software. The freeform selection tool was used to circumscribe the whole dorsal side of the heart (considered to be the total heart size) and/or the area covered by coronary vessels. The percentage of each individual heart covered by coronary vessels was used to assess the extent of coronary growth.

Tissue samples

Fetal heart tissue was procured from medical waste (StemExpress). Three samples were analyzed, which all displayed the same characteristics.

Statistics

All measurements were compiled, plotted, and analyzed using Prism 6 (GraphPad). Two-tailed, unpaired parametric *t* tests with Welch's correction were used to determine the *P* value for comparisons between groups. A *P* value of less than 0.05 was considered significant. Linear regression analysis was performed to measure the strength of association between 2 variables.

Study approval

All animal experiments performed at Stanford University, at the University of Helsinki, and at the Shanghai Institute for Biological Sciences (SIBS) were conducted in accordance with guidelines of the Stanford University Institutional Animal Care and Use Committee, the Committee for Animal Experiments of the District of Southern Finland, and the SIBS Institutional Animal Care and Use Committee, respectively. All human tissues were obtained with informed consent and used in a manner approved by the Stanford University Institutional Review Board.

Acknowledgments

We thank Sylvia Evans (*Isl1*), Lucile Miquerol (*Vegfa-lacZ*), Annette Damert (*Vegfa-lacZ*), Andras Nagy (*Vegfa-lacZ*), Brian Black (*Mef-2c-AHF-Cre*), and Louisa Iruela-Arispe (*VE-cadherin-CreER*) for mouse strains. H.I. Chen was partially supported by a summer research grant administered by the Stanford University Vice Provost for Undergraduate Education. B. Zhou is supported by the Ministry of Science and Technology (2013CB945302 and 2012CB945102) and the National Natural Science Foundation of China (91339104, 31271552, 31222038). J.C. Wu is supported by the NIH (R01 HL093172) and the American Heart Association Established Investigator Award. K. Red-Horse is supported by the NIH (4R00HL10579303) and the Searle Foundation.

Address correspondence to: Kristy Red-Horse, Gilbert Hall, 371 Serra Mall, Stanford, California 94305, USA. Phone: 650.724.3135; E-mail: kredhors@stanford.edu.

1. Zeina AR, Blinder J, Sharif D, Rosenschein U, Barmeir E. Congenital coronary artery anomalies in adults: non-invasive assessment with multidetector CT. *Br J Radiol*. 2009;82(975):254–261.
2. Angelini P. Coronary artery anomalies: an entity in search of an identity. *Circulation*. 2007;115(10):1296–1305.
3. Wesselhoeft H, Fawcett JS, Johnson AL. Anomalous origin of the left coronary artery from the pulmonary trunk. Its clinical spectrum, pathology, and pathophysiology, based on a review of 140 cases with seven further cases. *Circulation*. 1968;38(2):403–425.
4. Ginde S, Earing MG, Bartz PJ, Cava JR, Tweddell JS. Late complications after Takeuchi repair of anomalous left coronary artery from the pulmonary artery: case series and review of literature. *Pediatr Cardiol*. 2012;33(7):1115–1123.
5. Olivey HE, Svensson EC. Epicardial-myocardial signaling directing coronary vasculogenesis. *Circ Res*. 2010;106(5):818–832.
6. Bogers AJ, Gittenberger-De Groot AC, Poelmann RE, Péault BM, Huysmans HA. Development of the origin of the coronary arteries, a matter of ingrowth or outgrowth? *Anat Embryol*. 1989;180(5):437–441.
7. Waldo KL, Willner W, Kirby ML. Origin of the proximal coronary artery stems and a review of ventricular vascularization in the chick embryo. *Am J Anat*. 1990;188(2):109–120.

8. Ando K, Nakajima Y, Yamagishi T, Yamamoto S, Nakamura H. Development of proximal coronary arteries in quail embryonic heart: multiple capillaries penetrating the aortic sinus fuse to form main coronary trunk. *Circ Res*. 2004;94(3):346–352.
9. Riley PR, Smart N. Vascularizing the heart. *Cardiovasc Res*. 2011;91(2):260–268.
10. Hutchins GM, Kessler-Hanna A, Moore GW. Development of the coronary arteries in the embryonic human heart. *Circulation*. 1988;77(6):1250–1257.
11. Pérez-Pomares J-M, et al. Origin of coronary endothelial cells from epicardial mesothelium in avian embryos. *Int J Dev Biol*. 2002;46(8):1005–1013.
12. Tian X, et al. Peritruncal coronary endothelial cells contribute to proximal coronary artery stems and their aortic orifices in the mouse heart. *PLoS One*. 2013;8(11):e80857.
13. Tomanek RJ, et al. VEGF family members regulate myocardial tubulogenesis and coronary artery formation in the embryo. *Circ Res*. 2006;98(7):947–953.
14. Tomanek RJ, Hansen HK, Christensen LP. Temporally expressed PDGF and FGF-2 regulate embryonic coronary artery formation and growth. *Arterioscler Thromb Vasc Biol*. 2008;28(7):1237–1243.
15. Dyer L, Wu Y, Moser M, Patterson C. BMPER-induced BMP signaling promotes coronary artery remodeling. *Dev Biol*. 2014;386(2):385–394.
16. Waldo KL, Kumiski DH, Kirby ML. Association of the cardiac neural crest with development of the coronary arteries in the chick embryo. *Anat Rec*. 1994;239(3):315–331.
17. Ward C, Stadt H, Hutson M, Kirby ML. Ablation of the secondary heart field leads to tetralogy of Fallot and pulmonary atresia. *Dev Biol*. 2005;284(1):72–83.
18. Théveniau-Ruissy M, et al. The del22q11.2 candidate gene Tbx1 controls regional outflow tract identity and coronary artery patterning. *Circ Res*. 2008;103(2):142–148.
19. Li Wei, et al. An essential role for connexin43 gap junctions in mouse coronary artery development. *Development*. 2002;129(8):2031–2042.
20. González-Iriarte M, et al. Development of the coronary arteries in a murine model of transposition of great arteries. *J Mol Cell Cardiol*. 2003;35(7):795–802.
21. Ratajska A, Złotorowicz R, Błazejczyk M, Wasiutyñski A. Coronary artery embryogenesis in cardiac defects induced by retinoic acid in mice. *Birth Defects Res Part A Clin Mol Teratol*. 2005;73(12):966–979.
22. Chiu IS, et al. Evolution of coronary artery pattern according to short-axis aortopulmonary rotation: a new categorization for complete transposition of the great arteries. *J Am Coll Cardiol*. 1995;26(1):250–258.
23. Zhou B, et al. Fog2 is critical for cardiac function and maintenance of coronary vasculature in the adult mouse heart. *J Clin Invest*. 2009;119(6):1462–1476.
24. Heineke J, et al. Cardiomyocyte GATA4 functions as a stress-responsive regulator of angiogenesis in the murine heart. *J Clin Invest*. 2007;117(11):3198–3210.
25. Red-Horse K, Ueno H, Weissman IL, Krasnow MA. Coronary arteries form by developmental reprogramming of venous cells. *Nature*. 2010;464(7288):549–553.
26. Chen HI, et al. The sinus venosus contributes to the coronary vasculature through VEGF-C stimulated angiogenesis. *Development*. In press.
27. Wu B, et al. Endocardial cells form the coronary arteries by angiogenesis through myocardial-endocardial VEGF signaling. *Cell*. 2012;151(5):1083–1096.
28. Katz TC, et al. Distinct compartments of the proepicardial organ give rise to coronary vascular endothelial cells. *Dev Cell*. 2012;22(3):639–650.
29. Kivelä R, et al. VEGF-B-induced vascular growth leads to metabolic reprogramming and ischemia resistance in the heart. *EMBO Mol Med*. 2014;6(3):307–321.
30. Kärpanen T, et al. Overexpression of vascular endothelial growth factor-B in mouse heart alters cardiac lipid metabolism and induces myocardial hypertrophy. *Circ Res*. 2008;103(9):1018–1026.
31. Bellomo D, et al. Mice lacking the vascular endothelial growth factor-B gene (Vegfb) have smaller hearts, dysfunctional coronary vasculature, and impaired recovery from cardiac ischemia. *Circ Res*. 2000;86(2):E29–E35.
32. Li X, et al. Reevaluation of the role of VEGF-B suggests a restricted role in the revascularization of the ischemic myocardium. *Arterioscler Thromb Vasc Biol*. 2008;28(9):1614–1620.
33. Miquerol L, Gertsenstein M, Harpal K, Rossant J, Nagy A. Multiple developmental roles of VEGF suggested by a LacZ-tagged allele. *Dev Biol*. 1999;212(2):307–322.
34. Watanabe Y, Buckingham M. The formation of the embryonic mouse heart. *Ann N Y Acad Sci*. 2010;1188(1):15–24.
35. Laugwitz K-L, Moretti A, Caron L, Nakano A, Chien KR. Islet1 cardiovascular progenitors: a single source for heart lineages? *Development*. 2008;135(2):193–205.
36. Cai C-L, et al. Isl1 identifies a cardiac progenitor population that proliferates prior to differentiation and contributes a majority of cells to the heart. *Dev Cell*. 2003;5(6):877–889.
37. Verzi MP, McCulley DJ, De Val S, Dodou E, Black BL. The right ventricle, outflow tract, and ventricular septum comprise a restricted expression domain within the secondary/anterior heart field. *Dev Biol*. 2005;287(1):134–145.
38. Engleka KA, et al. Insertion of Cre into the Pax3 locus creates a new allele of Splotch and identifies unexpected Pax3 derivatives. *Dev Biol*. 2005;280(2):396–406.
39. Yamanaka O, Hobbs RE. Coronary artery anomalies in 126,595 patients undergoing coronary arteriography. *Cathet Cardiovasc Diagn*. 1990;21(1):28–40.
40. Maron BJ, et al. Recommendations and considerations related to preparticipation screening for cardiovascular abnormalities in competitive athletes: 2007 update: a scientific statement from the American Heart Association Council on Nutrition, Physical Activity, and Metabolism: endorsed by the American College of Cardiology Foundation. *Circulation*. 2007;115(12):1643–1655.
41. Eckart RE, et al. Sudden death in young adults: a 25-year review of autopsies in military recruits. *Ann Intern Med*. 2004;141(11):829–834.
42. Angelini P. Novel imaging of coronary artery anomalies to assess their prevalence, the causes of clinical symptoms, and the risk of sudden cardiac death. *Circ Cardiovasc Imaging*. 2014;7(4):747–754.
43. Yau JM, Singh R, Halpern EJ, Fischman D. Anomalous origin of the left coronary artery from the pulmonary artery in adults: a comprehensive review of 151 adult cases and a new diagnosis in a 53-year-old woman. *Clin Cardiol*. 2011;34(4):204–210.
44. Frescura C, et al. Anomalous origin of coronary arteries and risk of sudden death: a study based on an autopsy population of congenital heart disease. *Hum Pathol*. 1998;29(7):689–695.
45. Tomanek RJ, Ratajska A, Kitten GT, Yue X, Sandra A. Vascular endothelial growth factor expression coincides with coronary vasculogenesis and angiogenesis. *Dev Dyn*. 1999;215(1):54–61.
46. Gerber HP, et al. VEGF is required for growth and survival in neonatal mice. *Development*. 1999;126(6):1149–1159.
47. Liu H, et al. Role of VEGF and tissue hypoxia in patterning of neural and vascular cells recruited to the embryonic heart. *Dev Dyn*. 2009;238(11):2760–2769.
48. Giordano FJ, et al. A cardiac myocyte vascular endothelial growth factor paracrine pathway is required to maintain cardiac function. *Proc Natl Acad Sci U S A*. 2001;98(10):5780–5785.
49. Lavine KJ, Long F, Choi K, Smith C, Ornitz DM. Hedgehog signaling to distinct cell types differentially regulates coronary artery and vein development. *Development*. 2008;135(18):3161–3171.
50. Lavine KJ, et al. Fibroblast growth factor signals regulate a wave of Hedgehog activation that is essential for coronary vascular development. *Genes Dev*. 2006;20(12):1651–1666.
51. Dor Y, et al. A novel role for VEGF in endocardial cushion formation and its potential contribution to congenital heart defects. *Development*. 2001;128(9):1531–1538.
52. Chang C-P, et al. A field of myocardial-endocardial NFAT signaling underlies heart valve morphogenesis. *Cell*. 2004;118(5):649–663.
53. Stankunas K, Ma GK, Kuhnert FJ, Kuo CJ, Chang C-P. VEGF signaling has distinct spatiotemporal roles during heart valve development. *Dev Biol*. 2010;347(2):325–336.
54. Wikenheiser J, Doughman Y-Q, Fisher SA, Watanabe M. Differential levels of tissue hypoxia in the developing chicken heart. *Dev Dyn*. 2006;235(1):115–123.
55. Patten IS, et al. Cardiac angiogenic imbalance leads to peripartum cardiomyopathy. *Nature*. 2012;485(7398):333–338.
56. Yoshioka M, et al. Chondromodulin-I maintains cardiac valvular function by preventing angiogenesis. *Nat Med*. 2006;12(10):1151–1159.
57. Mundel TM, Kalluri R. Type IV collagen-derived angiogenesis inhibitors. *Microvasc Res*. 2007;74(2–3):85–89.
58. Kelly RG. The second heart field. *Curr Top Dev Biol*. 2012;100:33–65.
59. Bajolle F, et al. Rotation of the myocardial wall of the outflow tract is implicated in the normal positioning of the great arteries. *Circ Res*.

2006;98(3):421–428.
60. Karkkainen MJ, et al. Vascular endothelial growth factor C is required for sprouting of the first lymphatic vessels from embryonic veins. *Nat Immunol*. 2004;5(1):74–80.
61. Sun Y, et al. Islet 1 is expressed in distinct cardiovascular lineages, including pacemaker and coronary vascular cells. *Dev Biol*. 2007;304(1):286–296.
62. Monvoisin A, Alva JA, Hofmann JJ, Zovein AC, Lane TF, Iruela-Arispe ML. VE-cadherin-CreERT2 transgenic mouse: a model for inducible recombination in the endothelium. *Dev Dyn*. 2006;235(12):3413–3422.
63. Tian X, et al. Vessel formation. De novo formation of a distinct coronary vascular population in neonatal heart. *Science*. 2014;345(6192):90–94.
64. Sheikh AY, et al. In vivo genetic profiling and cellular localization of apelin reveals a hypoxia-sensitive, endothelial-centered pathway activated in ischemic heart failure. *Am J Physiol Heart Circ Physiol*. 2008;294(1):H88–H98.
65. Sharan SK, Thomason LC, Kuznetsov SG, Court DL. Recombineering: a homologous recombination-based method of genetic engineering. *Nat Protoc*. 2009;4(2):206–223.
66. Warming S, Costantino N, Court DL, Jenkins NA, Copeland NG. Simple and highly efficient BAC recombineering using galK selection. *Nucleic Acids Res*. 2005;33(4):e36.